Mathematical Modeling of Supercritical Extraction of Sage Oil

E. Reverchon
Dipt. di Ingegneria Chimica e Alimentare, Università di Salerno, 84084 Fisciano (SA), Italy

Modeling of supercritical CO_2 extraction of essential oils from leaves was studied using sage at 90 bar (9 MPa) and 50°C. The fractional separation of the extracts enabled essential oil to be obtained. Four mean sage particle sizes ranging from 0.25 to 3.10 mm were tested. The model proposed was based on differential mass balances performed along the extraction bed. Experimental data suggest that the internal mass transfer was the controlling stage for the extraction process. Different hypotheses were tested on vegetable matter geometry, and their incidence on the model performance was evaluated. The particle shape proved to be a key factor in fitting experimental results, which were fairly good when the conventional spherical geometry was replaced by a realistic slab geometry. Diffusivity of the solute in the solid matrix was used as the only adjustable parameter of the model; its best fit value was 6.0×10^{-13} m^2/s. The effect of the introduction of particle-size distribution into calculations was also tested. To verify if the external mass-transfer mechanisms influence the extraction process, experiments at two different CO_2 flow rates were also performed. Simplified models were also considered, and the extent of approximations was evaluated.

Introduction

The broad interest in supercritical CO_2 extraction (SFE) of essential oils is proved by the large number of scientific literature published on this argument (Stahl et al., 1987; Moyler, 1993). These studies were undertaken in view of a possible industrial application of the process. Indeed, unlike classical techniques, SFE can potentially produce improved fragrances: no thermal degradation and no pollution of the extracts is present, whereas steam distillation (SD) and solvent extraction (SE) processes are affected by one or both of these problems.

To design an extraction plant, it is necessary to have reliable mass-transfer models that will allow the determination of optimum operating conditions. Nevertheless, only a few attempts have been performed to model the SFE of essential oils. This is probably due to the complexity of the vegetable structure and to the lack of reliable experimental data on the yield of the process and on the influence of the solvent flow rate and of particle size. SFE performed by single stage extraction and separation produces the simultaneous extraction of several compound families that provide a quasi-solid extract. Indeed, hydrocarbon terpenes, oxygenated terpenes, and other related products that constitute essential oil are extracted together with paraffins and other undesired compounds. Consequently, yield data are biased by the presence of undesired compounds that modify both the measured yield and the shape of the extraction curve. Therefore, a fractional separation of the extracts is required (Stahl et al., 1987; Reverchon, 1992; Reverchon and Senatore, 1992). This process arrangement is necessary to produce extracts whose chemical, physical, and organoleptic properties are similar to those of essential oils (Reverchon and Senatore, 1992; Reverchon et al., 1994a).

Some authors have attempted to describe the evolution of the extraction process by using empirical kinetic equations (Spiro and Kandiah, 1990; Nguyen et al., 1991).

A second kind of model was based on the analogy between the heat and mass transfer. All particles were assumed to be spherical and the equations that apply to the cooling of a "hot ball" in a uniform medium were used to describe the concentration profile inside the particles as a function of time (Bartle et al., 1990; Reverchon et al., 1993a; Reverchon et al., 1994b). The model considered all particles at the same extraction conditions, i.e., the extractor volume was considered as a lumped parameter.

Other authors have proposed models based on differential mass balances along the extraction bed. To integrate the differential equations these models require information on the mass-transfer mechanism that characterizes the extraction process and data on the equilibrium relationship. Goto et al. (1993) studied SFE of peppermint oil assuming that the essential oil was adsorbed on lipids located on the surface of leaves, and developed their model according to this hypothesis. They concluded that the adsorption equilibrium alone controlled the overall extraction rate. Sovovà et al. (1994a) analyzed SFE of caraway seed essential oil. Their assumption was that the essential oil was mixed with the vegetable oil and was in part directly exposed to the solvent in cells broken up by milling. These authors developed a model that divided the process in two parts: the first was dominated by external mass-transfer resistance and the second one was dominated by internal mass-transfer resistance. Reverchon and Sesti Ossèo (1994) proposed a fitting of the experimental results of SFE of basil essential oil. The model neglected the concentration profile along the bed and the accumulation in the fluid phase. Nevertheless, it was successfully tested for different mean particle sizes. A fair fitting was obtained by introducing the experimental particle-size distribution in the model computations.

In spite of the various modeling approaches, the major problem in SFE of essential oils is to obtain extraction data not biased by the coextraction of unwanted compounds. The low reliability of the experimental data also affects the validity of the model proposed.

This work aimed at two main objectives. First, to produce accurate experimental data on SFE of sage essential oil, avoiding coextraction of waxes and other undesired compounds. To obtain this objective, experiments were performed at optimum extraction pressure and temperature as shown by a previous work (Reverchon, 1995). Moreover, the fractional separation of extracts was applied (Reverchon, 1992). The evolution of the oil yield with the extraction time was then monitored for different particle sizes and CO_2 flow rates.

Secondly, on the basis of the experimental results, a reliable model of the SFE process was developed. A model based on the integration of differential mass balances written along the extraction bed was proposed. Different sage particles geometries were tested since the conventional spherical geometry failed to fit the experimental data.

Experimental Studies

Sage leaves (*Salvia officinalis*, L.) air dried in the shade, were supplied by Betulla srl (Italy). When received, the leaves had a moisture content of 9.6% by weight on dry basis. They were grinded mechanically, and care was taken to avoid heating the vegetable material.

The experimental apparatus consisted of a Milroyal B (Milton Roy) high-pressure pump that delivered CO_2 to a thermostated extraction vessel (400 cm^3 internal volume, 16.5 cm height) in which about 0.16 kg of dried sage particles were charged. The solution at the exit of the extractor flowed into two 200 cm^3 series-operated separators. Their operating conditions were set at a pressure and temperature suitable to obtain the precipitation of the different compound families extracted. The CO_2 flow rate and total volume were measured at the exit of the apparatus by a calibrated rotameter (Matheson mod. 304) and a dry test meter (Sim Brunt mod. B10), respectively. Greater details on the experimental apparatus used can be found in previous works (Reverchon, 1992; Reverchon et al., 1993).

Most extraction tests were performed at a CO_2 flow rate of 0.95 kg/h. Further tests were performed at a CO_2 flow rate of 0.53 kg/h on a 0.75 mm mean diameter sage particle charge to assess the influence of the solvent flow rate on the extraction process.

The mean particle size was evaluated by mechanical sieving. Batches of 3.10, 0.75, 0.50 and 0.25 mm mean particle sizes were used.

Samples of sage particles were observed under optical microscopy. The majority of the particles whose diameter was under about 0.4 mm diameter showed a quasi-spherical shape, whereas, for larger particles the flat structure of the sage leaves was largely preserved. These particles can be better described as irregular slabs or cylinders whose height is 0.29 mm. This value represents the mean thickness of dried sage leaves measured by a micrometer.

SFE experiments were performed at a pressure of 90 bar (9 MPa) and at a temperature of 50°C. These process conditions provided the optimum sage oil composition since higher molecular weight compounds, except waxes, were not extracted (Reverchon et al., 1995). Two separators were operated at a pressure of 85 bar (8.5 MPa) and a temperature of -12°C, and at a pressure of 17 bar (1.7 MPa) and a temperature of -6°C, respectively. These operating conditions allowed a complete separation of waxes which precipitated in the first separator, whereas the components of sage essential oil were separated in the second separator. This selective separation is not feasible during extraction since cuticular waxes are located on the leaf surface. Therefore, waxes are first extracted during SFE despite their lower solubility compared to the solubility of essential oil compounds.

The high performance of the separation of cuticular waxes and the high quality of the oil were confirmed by GC-MS peak identification performed on the products collected in the separators (Reverchon et al., 1995). The two main oil compounds resulted to be 1–8 cineole (54.4%) and caryophyllene (7.1%). However, all the other compounds constituting the extract belonged to the hydrocarbon or oxygenated terpenes and sesquiterpenes family. Waxes were mainly formed by *n*-paraffins ranging from C_{25} to C_{33}.

The extraction yield was measured by weighing the solute collected in the second separator at fixed time intervals. The asymptotic essential oil yield was 1.35% by weight of the charged material. The initial oil concentration in the solid phase was 9.0 kg/m^3. The asymptotic wax yield was 0.2% by weight at the optimum extraction conditions.

Extraction Model

Botanical books indicate that terpenoids constituting essential oil can be mainly located inside the vegetable cells in organules called vacuoles (Pridham, 1967). Only a small fraction of essential oil might be near the particle surface due to the breaking up of cells during grinding or in epidermal hairs located on the leaf surface. Therefore, the hypothesis formu-

lated by Goto et al. (1993) that essential oil is adsorbed on leaf waxes seems not to be supported by the configuration of the vegetable matter that appears from this analysis. The fraction of oil freely available on the particle surface should not be significant in the case of SFE from leaves. Indeed, this hypothesis is justified only for SFE of seed oils (Sovovà et al., 1994b; Bulley et al., 1984; Lee et al., 1986) due to the structure of seeds and their very high content of oil (up to 50% by weight of the vegetable material). Consequently, SFE of essential oil from leaves should be mainly controlled by the internal mass-transfer resistance. Therefore, the external mass-transfer coefficient was neglected in the development of the model.

Due to the similarity of the extracted compounds collected in the second separator, essential oil will be considered as a single compound. The mass balances were developed in the additional hypotheses that the axial dispersion can be neglected and that the solvent density and flow rate are constant along the bed. Thus, the mass balances over an element of the extractor of height dh can be written as

$$uV\frac{\partial c}{\partial h} + \epsilon V\frac{\partial c}{\partial t} + (1-\epsilon)V\frac{\partial \bar{c}}{\partial t} = 0 \tag{1}$$

$$(1-\epsilon)V\frac{\partial \bar{c}}{\partial t} = -A_p K(\bar{c} - \bar{c}^*) \tag{2}$$

IC at $t = 0$, $c = 0$ and $\bar{c} = \bar{c}_0$;
BC at $h = 0$, $c(0, t) = 0$.

where ϵ is the bed porosity, V is the extractor volume (m^3), c is the extract concentration in the fluid phase (kg/m^3), $\bar{c}$ is the extract concentration in the solid phase (kg/m^3), u is the superficial solvent velocity (m/s), A_p is the total surface of particles (m^2), $\bar{c}^*$ is the concentration at the solid-fluid interface which according to the internal resistance model is supposed to be at equilibrium with the fluid phase (kg/m^3), h is the spatial coordinate along the bed (m), t is the extraction time (s), $\bar{c}_0$ is the initial concentration in the solid phase (kg/m^3), and K (m/s) is the internal mass-transfer coefficient.

Mass balances 1, 2 can be solved if the solid vs. liquid-phase equilibrium relationship $\bar{c}^*$ (c) is known. As a rule, a linear relationship is used for SFE processes due to the lack of experimental phase equilibrium data

$$c = k_p \cdot \bar{c}^* \tag{3}$$

where k_p is the volumetric partition coefficient of the extract between the solid and the fluid phase at equilibrium.

Until now, no hypothesis has been formulated on the geometry of vegetable particles. In the majority of the models found in the literature (see introduction), particles are assumed to be spherical. Indeed, many particulate matters conform well with this representation.

In Eq. 2 the group $A_pK/(1-\epsilon)V$ depends on the geometry of particles through A_pK, and ϵ is supposed to be constant within the bed. This group is dimensionally equal to 1/s. Therefore, it is possible to define $t_i = (1-\epsilon)V/A_pK$ where t_i is the internal diffusion time which, according to the above hypotheses, is characteristic of the extraction process.

Therefore, Eq. 2 can be rewritten as

$$\frac{\partial \bar{c}}{\partial t} = -\frac{1}{t_i}(\bar{c} - \bar{c}^*) \tag{4}$$

In a more general context, Villermaux (1987) showed the equivalence between the diffusion time and the internal diffusion coefficient D_i for different particle geometries. He proposed the following relationship

$$t_i = \mu\frac{l^2}{D_i} \tag{5}$$

where μ is a coefficient depending on particle geometry. In the case of spherical particles μ is equal to 3/5. For cylinders and slabs it is equal to 1/2 and to 1/3, respectively. $l = V_p/A_p$ (particle volume/particle surface) is a characteristic dimension. l is equal to $r/3$ for spherical particles where r is the mean particle radius.

The equations system 1, 4 with the equilibrium relationship 3 is hyperbolic, and with the proposed boundary and initial conditions it can be numerically solved by using the method of characteristics. In an alternative to this method the fixed bed can be divided in n stages. In each stage the fluid and solid phase composition is considered to be uniform. This representation approximates the description of a plug-flow extractor through a series of mixed extractors. Thus, Eqs. 1 and 4 can be rewritten as a set of $2n$ equations

$$\frac{W}{\rho}(c_n - c_{n-1}) + \epsilon\frac{V}{n}\frac{dc_n}{dt} + \left[(1-\epsilon)\frac{V}{n}\right]\frac{d\bar{c}_n}{dt} = 0 \tag{6}$$

$$\frac{d\bar{c}_n}{dt} = -\frac{1}{t_i}(\bar{c}_n - \bar{c}_n^*) \tag{7}$$

with the initial conditions at $t = 0$, $\bar{c}_n = 0$ and $c_n = 0$, where W is the CO_2 mass flow rate (kg/s), ρ is the solvent density (kg/m^3), $\bar{c}_n$ is the solid phase concentration in the nth stage (kg/m^3), c_n is the fluid-phase concentration in the nth stage (kg/m^3), and n is the number of stages deriving from the bed subdivision.

The higher the number of stages, the better the behavior of the PDEs (Eqs. 1 and 4) can be approximated by the system of ODEs (Eqs. 6 and 7). The advantage of this formulation is that Eqs. 6 and 7 can be numerically solved by using a fourth-order Runge-Kutta method. This numerical method can be easily implemented on many commercial mathematical software packages. It only requires a somewhat larger memory usage than the method of characteristics.

In the limited case of $n = 1$ the whole extractor is assumed to have the same phase concentration. This is one of the most widely used simplified representations of the supercritical extraction process.

In the hypothesis that the extraction time is much larger than the residence time ($V\rho\epsilon/W$) it is also possible to further simplify the model assuming $dc/dt = 0$, i.e., to affirm that the accumulation in the fluid phase is negligible. In this case a previously analyzed analytical solution exists (Reverchon and Sesti Ossèo, 1994).

Modeling Results and Discussion

A value of the partition factor of essential oil between phases (k_p) is required to solve the system of mass balance equations. Experimental data on the partition factor between vegetable matter and supercritical CO_2 was given by Spiro and Kandiah (1990) that evaluated it for the extraction of ginger oleoresin from ginger rhizomes. They monitored the concentration of a characteristic ginger compound ([6] gingerol) in the fluid and in the solid phase, obtaining a mean mass partition factor (k_m) of 0.29. According to these authors k_m can be converted in k_p as follows

$$k_p = \frac{k_m \rho}{\rho_s} \tag{8}$$

where ρ_s is the solid density. Following this indication a k_p value of about 0.2 was applied at our operating conditions.

A comparison was first performed between the concentration profiles predicted by the equations system 1 and 4, integrated by the method of characteristics, and the equations system 6 and 7, integrated by the fourth-order Runge-Kutta method. This last equation system was integrated for different values of n. For SFE of sage oil at optimum extraction conditions and for $n = 10$, the two models showed concentration profiles that were indistinguishable. Therefore in the following, the numerical analysis was performed by using equation system 6, 7, in which the bed divided into ten stages. This case was assumed as the basis for discussion.

In a first data modeling attempt the particles were considered spherical. Indeed, this assumption is the most widely adopted in the literature even when the materials treated do not conform to this geometry. The result was unsatisfactory (see Figure 1). A value of D_i of 6.0×10^{-13} (m^2/s) was used to fit the experimental results for particles whose mean diameter was 0.25 mm. The same D_i value was used to calculate all the other curves in Figure 1 that were produced for particle diameters up to 3.1 mm. These curves showed a large and increasing overestimation of the influence of the particle size on the mass-transfer process, i.e., the deviation of the model curves from the experimental points increased with the increase in the particle size. A possible explanation is that the description of the particle geometry was not correct, i.e., an incorrect value for the V_p/A_p ratio was used. While spherical geometry is reasonable for small leaf particles (0.25 and 0.50 mm), this assumption can be far less justified when larger particles are considered. Indeed, as observed under optical microscopy, larger sage particles were flat rather than spherical. Thus, the geometry of sage particles can be more reasonably represented by slabs. This geometry was therefore introduced in the calculation. The measured mean thickness of sage leaves (0.29 mm) was assumed as the height of the slab particles. The other two dimensions of the slab were assumed to be equal to the mean particle size of the charge when measured by sieving. According to this assumption, all sage particles had the same height, whereas the other two dimensions were determined by the extent of the grinding. The V_p/A_p ratio for these slabs was then calculated and the fitting of experimental results to the model equations was once again performed. A fairly good fitting was obtained for the whole range of particle sizes studied. The best fit among the yield curves and the experimental data was obtained for $D_i =$

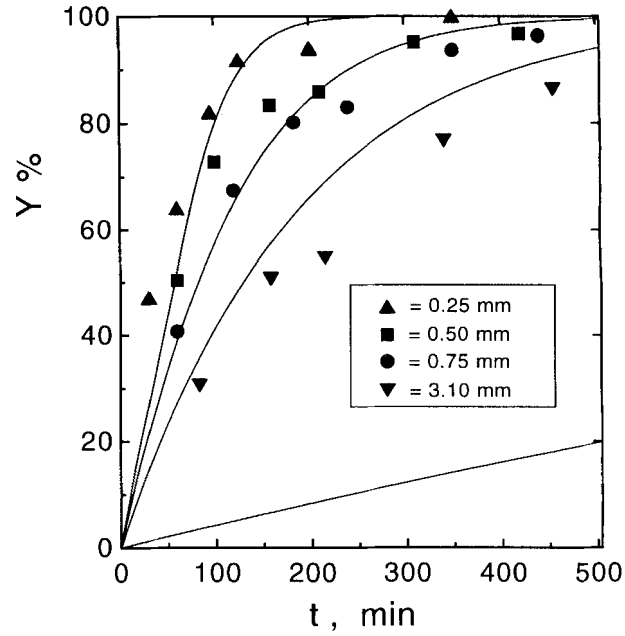

Figure 1. First attempt at fitting SFE data by using Eqs. 6 and 7 (continuous lines).

Spherical sage particles were assumed; $Di = 6.0\times10^{-13}$ m^2/s.

6.0×10^{-13} m^2/s (Figure 2). The fitting was particularly good even when considering the largest sage particles treated (3.10 mm).

In Figures 3 and 4 predicted essential oil concentration in the solid and in the fluid phase, as a function of the distance from the bed entrance and of the extraction time (for 0.50-mm particles), are reported, respectively. These diagrams show the progressive exhaustion of the vegetable matrix and the concentration profiles along the bed. Fluid-phase concentration is always very low when compared to the solid-phase concentration. This behavior will be more evident for larger particle sizes.

The hypothesis that the internal diffusion is the limiting stage of the mass-transfer mechanism was further verified by performing SFE of sage oil at different CO_2 flow rates. Indeed, if the extraction yield depends on the external mass-transfer mechanism it would change by varying the solvent flow rate. The oil yield obtained for 0.75-mm particles is reported in Figure 5a against the extraction time and in Figure 5b against the specific quantity of solvent used (m_s/m_o). The yield measured for the two series of runs performed at different CO_2 flow rates substantially overlaps when expressed against the extraction time, whereas it produces two distinct curves when expressed against the specific mass of solvent used. This confirms that the extraction process is controlled by the internal mass-transfer mechanism. For a fixed value of the mean particle size, the oil yield is only related to the extraction time. In other words, two different CO_2 flow rates produce a different solute loading of the supercritical solvent at the exit of the extractor but do not produce different extraction rates. A similar result was also described by Goto et al. (1994) for SFE of oleresin from ginger rhizome.

The effect of particle-size distribution (PSD) was also taken into account to attempt a further improvement in the de-

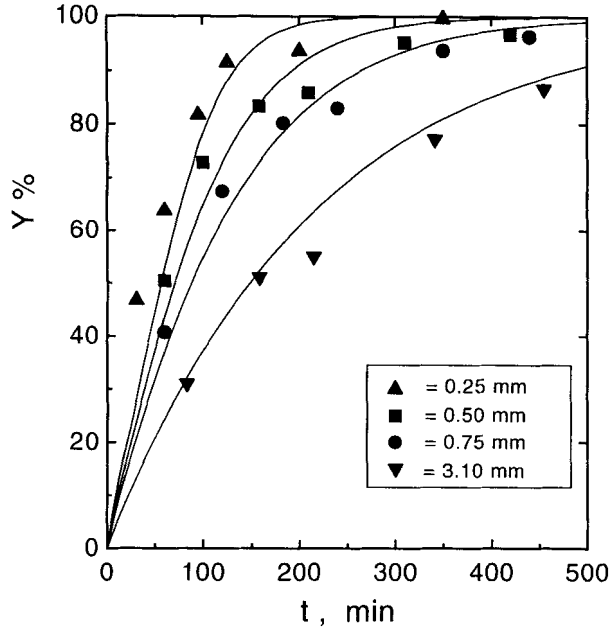

Figure 2. Best fit of sage SFE data by using Eqs. 6 and 7.

Sage particles were assumed as slabs whose height was equal to 0.29 mm that is the mean leaf thickness; $Di = 6.0 \times 10^{-13}$ m^2/s.

scription of experimental data. The yield curve (Y_i) was calculated by numerically solving the model equations for each particle fraction that constitutes the particle-size distribution. Then, the overall behavior of the charge (Y_{psd}) was obtained as

$$Y_{psd}(t) = \sum_i Y_i(t) \cdot p_i \qquad (9)$$

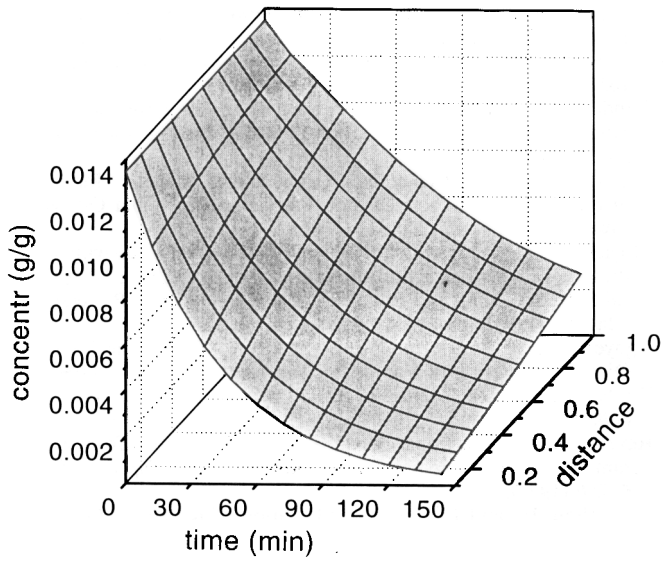

Figure 3. Predicted essential oil concentration in the solid phase as a function of the normalized distance from the bed entrance and time.

$Di = 6.0 \times 10^{-13}$ m^2/s; mean particle dimension = 0.50 mm.

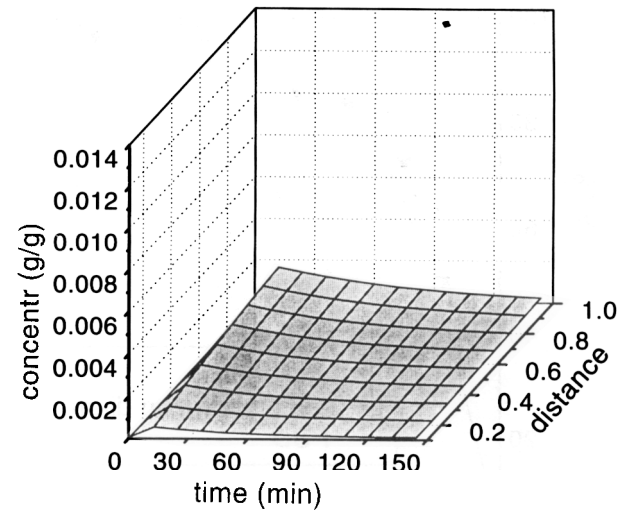

Figure 4. Predicted essential oil concentration in the fluid phase as a function of the normalized distance from the bed entrance and time.

$Di = 6.0 \times 10^{-13}$ m^2/s; mean particle dimension = 0.50 mm.

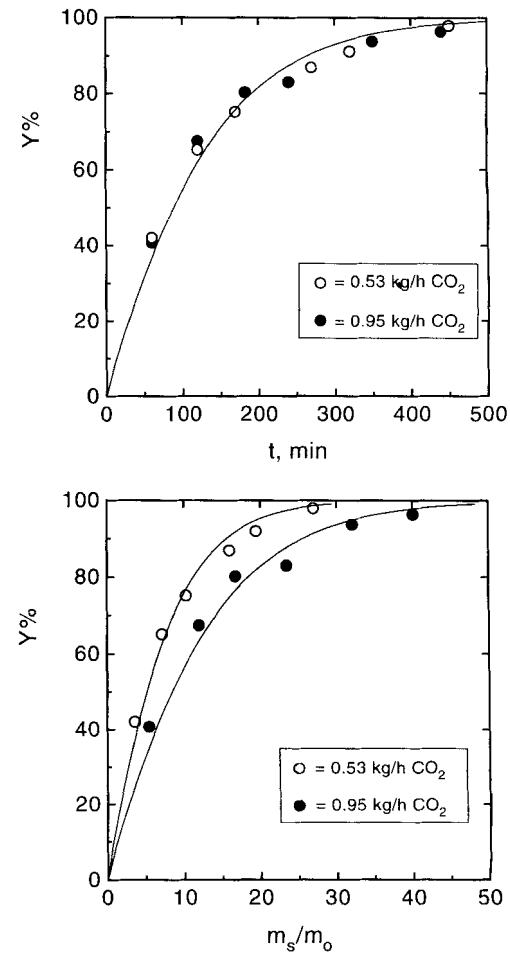

Figure 5. Yield of sage essential oil against (a) the extraction time by varying CO_2 flow rate; (b) the specific solvent ratio m_s/m_o by varying CO_2 flow rate.

Mean particle size = 0.75 mm.

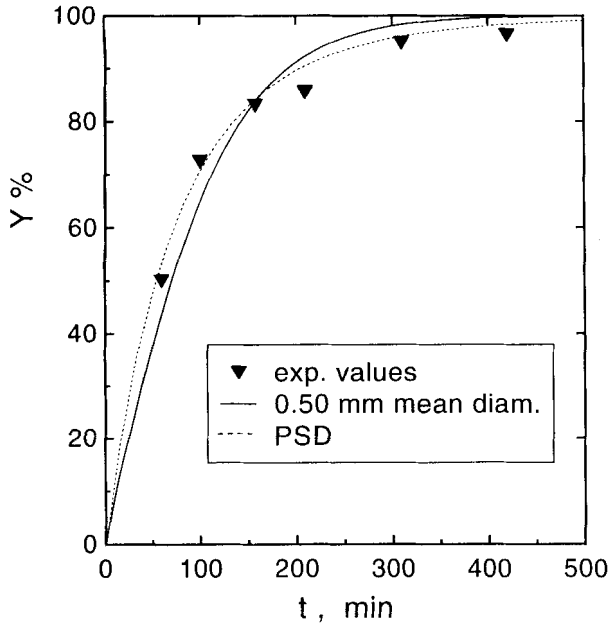

Figure 6. Yield of sage essential oil predicted by the Eqs. 6 and 7 when the mean particle size (0.50 mm) or the particle-size distribution is used in calculations.

where p_i is the percentage by weight of each fraction of the charge.

The introduction of particle-size distribution produces a modification of the shape of the predicted yield curve, as shown in Figure 6, in the case of 0.50-mm particles. The smallest particles determined an increase of the yield at the shorter extraction times with regard to the calculations performed by using the mean particle dimension. On the contrary, the largest particles required longer asymptotic times for the extraction. Similar effects were obtained for the other particle sizes studied, though the influence of particle-size distribution rapidly decreased with the increase in the mean particle size.

Thus, the overall effect of particle-size distribution introduction is an improved fitting of the experimental data for small particles. However, the analysis of the problem presents no substantial modifications, whereas very long calculations are required to take into account particle-size distribution.

The numerical integration of the system of ODEs 6, 7 for $n = 1$ was also performed. This solution is equivalent to the hypothesis that fluid-phase concentration is uniform all along the bed, i.e., concentration profiles in the fluid phase (Figure 4) can be neglected. The concentration curves obtained against the extraction time for particle sizes larger than 0.50 mm resulted in being very similar to those obtained for the base case. This means that the approximation introduced by this hypothesis could be acceptable for large particles.

The simplified model obtained by further imposing $dc/dt = 0$ in Eq. 6 was also explored. It produced a larger deviation of the predicted yield curve compared to the base case. In this case too, the deviation decreased with the increase in the diameter of the particles. The applicability of this hypothesis to SFE of essential oils was discussed extensively in a previous work (Reverchon and Sesti Ossèo, 1994).

The evidence obtained for the simplified models can be explained by comparing the internal diffusion time to the residence time. During SFE of essential oil, the internal diffusion times are generally very large compared to the residence time. For example, for a CO_2 flow rate of 0.95 kg/h, and for particles of 0.50 mm mean size, the residence time amounts to 440 s whereas the internal diffusion time is about 4,000 s.

Acknowledgment

The work was performed partly in the framework of Progetto Strategico "Tecnologie Chimiche Innovative," CNR, Rome, Italy.

Notation

$\bar{c}$ = extract concentration in the solid phase, kg/m^3
D_i = diffusion coefficient, m^2/s
$l = V_p/A_p$ particle volume/particle surface, m
m_o = mass of solute charged into the extractor, kg
m_s = mass of solvent flowed into the extractor, kg
t_i = internal diffusion time, s
Y_{psd} = cumulative extraction yield
Y_i = extraction yield for a single fraction of particles

Greek letter

ρ_s = solid phase density, kg/m^3

Literature Cited

Bartle, K. D., A. A. Clifford, S. B. Hawthorne, J. J. Langenfeld, D. J. Miller, and R. A. Robinson, "A Model for Dynamic Extraction Using a Supercritical Fluid," *J. Supercrit. Fluids*, **3**, 143 (1990).

Bulley, N. R., M. Fattori, A. Meisen, and L. Moyls, "Supercritical Fluid Extraction of Vegetable Oil Seeds," *JAOCS*, **61**, 1362 (1984).

Goto, M., M. Sato, and T. Hirose, "Extraction of Peppermint Oil by Supercritical Carbon Dioxide," *Japanese J. Chem. Eng.*, **26**(4), 401 (1993).

Goto, M., B. C. Roy, Y. Nomura, and T. Hirose, "Kinetic Studies of Supercritical Fluid Extraction from Natural Solid Materials," M. Perrut and G. Brunner, eds., *Proc. Symp. on Supercrit. Fluids*, Vol. 2, Strasbourg, France, INPL Inst. Nat. Polythec. de Lorraine, p. 165 (1994).

Kandiah, M., and M. Spiro, "Extraction of Ginger Rhizome: Kinetic Studies with Supercritical Carbon Dioxide," *Int. J. Food Sci. Tech.*, **25**, 328 (1990).

Lee, A. K. K., N. R. Bulley, M. Fattori, and A. Meisen, "Modelling of Supercritical Carbon Dioxide Extraction of Canola Oilseed in Fixed Beds," *JAOCS*, **63**, 921 (1986).

Moyler, D. A., "Extraction of Flavours and Fragrances with Compressed CO_2 in Extraction of Natural Products Using Near-Critical Solvents," King and Bott, eds., Blackie Academic Professional, Glasgow (1993).

Nguyen, K., P. Barton, and J. S. Spencer, "Supercritical Carbon Dioxide Extraction of Vanilla," *J. Supercrit. Fluids*, **4**, 40 (1991).

Pridham, J. B., *Terpenoids in Plants*, Academic Press, New York (1967).

Reverchon, E., "Fractional Separation of SFE Extracts from Marjoram Leaves: Mass Transfer and Optimization," *J. Supercrit. Fluids*, **5**, 256 (1992).

Reverchon, E., and F. Senatore, "Isolation of Rosemary Oil: Comparison Between Hydrodistillation and Supercritical CO_2 Extraction," *J. Flavour Fragr.*, **7**, 227 (1992).

Reverchon, E., G. Donsì, and L. Sesti Ossèo, "Modeling of Supercritical Fluid Extraction from Herbaceous Matrices," *Ind Eng. Chem. Res.*, **32**, 2721 (1993).

Reverchon, E., A. Ambruosi, and F. Senatore, "Isolation of Peppermint Oil Using Supercritical CO_2," *J. Flavour Fragr.*, **9**, 19 (1994a).

Reverchon, E., L. Sesti Ossèo, and D. Gorgoglione, "Supercritical CO_2 Extraction of Basil Oil: Characterization of Products and Process Modeling," *J. Supercrit. Fluids*, **7**, 185 (1994b).
Reverchon, E., and L. Sesti Ossèo, "Modelling the Supercritical Extraction of Basil Oil," *Proc. Symp. on Supercrit. Fluids*, Strasbourg, France, M. Perrut and G. Brunner, eds., **2**, p. 189 (1994).
Reverchon, E., G. Della Porta, and R. Taddeo, "Extraction of Sage Oil by Supercritical CO_2: Influence of Some Process Parameters," *J. Supercrit. Fluids*, **8**, 302 (1995).
Spiro, M., and M. Kandiah, "Extraction of Ginger Rhizome: Partition Constants and Other Equilibrium Properties in Organic Solvents and in Supercritical Carbon Dioxide," *Int. J. Food Sci. Tech.*, **25**, 566 (1990).
Stahl, E., K. W. Quirin, and D. Gerard, *Verdichtete Gase Zur Extraction und Raffination*, Springer Verlag, Berlin (1987).
Sovovà, H., R. Komers, J. Kucera, and J. Jez, "Supercritical Carbon Dioxide Extraction of Caraway Essential Oil," *Chem. Eng. Sci.*, **49**, 2499 (1994a).
Sovovà, H., J. Kucera, and J. Jez, "Rate of the Vegetable Oil Extraction with Supercritical CO_2: II Extraction of Grape Oil," *Chem. Eng. Sci.*, **49**, 415 (1994b).
Villermaux, J., "Chemical Engineering Approach to Dynamic Modelling of Linear Chromatography," *J. Chromatog.*, **406**, 11 (1987).

Manuscript received Dec. 15, 1994, and revision received Sept. 15, 1995.

Corrections

- In the R&D note titled "Correlation of Vapor-Liquid Equilibrium Ratio of Hydrogen" (June 1995, p. 1602), four pressure labels on Figure 1 (p. 1603) that read 1 MPa, 5 MPa, 10 MPa, and 15 MPa are incorrect and should be corrected to read 0.1 MPa, 1 MPa, 5 MPa, and 10 MPa, respectively. The highest pressure, 25 MPa, is correct and should remain unchanged.

- In the R&D note titled "Instability Phenomenon in an External-Loop Three-Phase Gas-Liquid-Solid Airlift Reactor" (November 1995, p. 2508), the first author's name of the third item in the Literature Cited section (p. 2511) should read Heijnen, S. J., not Heijen, S. J.